

Preparation of Colloidal Suspensions of Discrete TS-1 Crystals

Guangyu Zhang, Johan Sterte, and Brian J. Schoeman*

Department of Chemical Technology, Luleå University of Technology, S-971 87 Luleå, Sweden

Received May 28, 1996. Revised Manuscript Received September 17, 1996[®]

Stable colloidal suspensions containing discrete TS-1 crystals with average crystal sizes less than 100 nm and with a narrow particle size distribution have been synthesized from clear homogeneous solutions. The products were characterized with respect to crystallinity, crystal size and size distribution, Ti incorporation, specific surface areas, the nature of the Ti species in the products, and the colloidal crystals surface electric charge. The influence of several parameters including synthesis mixture composition and crystallization temperature on crystal size and Ti incorporation were investigated. The synthesis of colloidal crystals with an average size less than 100 nm is favored by low crystallization temperatures (100 °C), a highly basic environment, concentrated mixtures, and low Ti contents in the synthesis solutions. The maximum incorporation of tetrahedrally coordinated Ti was 0.84 mol %. High crystallization temperatures (>100 °C) favor products with a low Si/Ti molar ratio, but larger crystals are formed, >100 nm, and octahedrally coordinated Ti and extra-framework Ti are detected. A preliminary investigation of the clear hydrolyzed precursor solution and its freeze-dried amorphous equivalent showed that small particles with an average size of 4.8 nm exist in the solution and a certain degree of ordering resembling the MFI structure was present in the precursor particles.

Introduction

Molecular sieves (crystalline aluminosilicates) are currently used within fields such as the petrochemical industry (as cracking and re-forming catalysts), for selective sorption (e.g., H₂O) and as ion exchangers (detergent industry). Recently the possible applications of molecular sieves have been expanded to several other advanced areas such as supramolecular catalysis, photochemistry, nanochemistry, and electrochemistry.

TS-1, a member of the class of pentasils in the zeolite group, was first synthesized by Taramasso et al.¹ in 1983. In the past decade it has been intensively studied due to its interesting properties in heterogeneous oxidation catalysis. Isomorphous substitution of Ti as a T atom in high-silica ZSM-5 imparts unique oxidative and selective catalytic properties to TS-1. TS-1 is claimed to be an efficient catalyst for the epoxidation of alkenes,² hydroxylation of aromatics,³ oxidation of alcohols,⁴ ammoxidation of cyclohexanone,⁵ and oxygenation of alkanes^{6,7} under mild conditions. It is believed that the Ti in the TS-1 framework and the surrounding unique pore structure yields a high-performance, highly flexible, and very stable catalytic site. These three properties permit the catalysis of several oxidation reactions

as those listed above with high activity and selectivity.⁸ Among many parameters that can affect catalytic activity, crystal size has been shown to be a major factor since smaller TS-1 crystals show higher activity than larger crystals due to a reduction in pore diffusion resistance.⁹ Van der Pol et al. reported that the smallest TS-1 crystals synthesized in their work were 90 nm, but these small primary crystals were present as aggregates; the size of the secondary particles was a few millimeters.¹⁰

The preparation of zeolite films on different supports has aroused considerable interest due to the possible applications of these composite materials as separation membranes, catalysts, and sensors. Several possible and promising applications of the composite materials require, however, that the film be thin, <ca. 500 nm. The use of colloidal zeolite as a seeding sol in the preparation of ultrathin films and fiber coatings, <150 nm thick, has been shown to be an effective material for this purpose.¹¹ The synthesis of zeolite crystals in the form of stable colloidal suspensions and the factors influencing the crystallization, with the use of these materials for the preparation of ultrathin molecular sieve films in mind, is therefore a topic of great interest. Colloidal suspensions of for example silicalite-1,¹² zeolite N-Y and N-A,¹³ and ZSM-5,¹⁴ have been successfully synthesized in the past few years.

* To whom correspondence should be addressed.

[®] Abstract published in *Advance ACS Abstracts*, November 1, 1996.

(1) Taramasso, M.; Perego, G.; Notari, B. *U.S. Patent* 4,410,501, 1983.

(2) Clerici, M. G.; Bellussi, G.; Romano, U. *J. Catal.* **1991**, *129*, 159.

(3) Esposito, A.; Taramasso, M.; Neri, C.; Buonoanno, F. *U.K. Patent* 2,116,974, 1985.

(4) Esposito, A.; Neri, C.; Buonoanno, F. *U.S. Patent* 4,480,135, 1984.

(5) Roffia, P.; Leofanti, G.; Cesana, A.; Mantegazza, M.; Padovan, M.; Petrini, G.; Tonti, S.; Gervasutti, V.; Varagnolo, R. *Chim. Ind.* **1990**, *72*, 598.

(6) Tatsumi, T.; Nakamura, M.; Nagashi, S.; Tominaga, H. *J. Chem. Soc., Chem. Commun.* **1990**, 476.

(7) Huybrechts, D. R. C.; De Bruycker, L.; Jacobs, P. A. *Nature* **1990**, *345*, 240.

(8) Bellussi, G.; Fattore, V. *Stud. Surf. Sci. Catal.*, **1991**, *69*, 79.

(9) van der Pol, A. J. H. P.; Verduyn, A. J.; van Hooff, J. H. C. *Appl. Catal. A* **1992**, *92*, 113.

(10) van der Pol, A. J. H. P.; van Hooff, J. H. C. *Appl. Catal. A* **1992**, *92*, 93.

(11) Hedlund, J.; Schoeman, B. J.; Sterte, J. *Stud. Surf. Sci. Catal.*, in press.

(12) Persson, A. E.; Schoeman, B. J.; Sterte, J.; Otterstedt, J.-E. *Zeolites* **1994**, *14*, 557.

(13) Schoeman, B. J.; Sterte, J.; Otterstedt, J.-E. *Zeolites* **1994**, *14*, 110.

In this paper, we present the synthesis of discrete colloidal crystals of TS-1 and the characterization of the synthesis products. The influence of several factors on the synthesis of stable colloidal suspensions of TS-1 are reported.

Experimental Section

Materials. The silica source used in the syntheses of TS-1 was tetraethoxysilane (TEOS, >98%, <5 ppm Al, Aldrich-Chemie) and the titania source was tetraethyl orthotitanate, (TEOT, Sigma). The tetrapropylammonium hydroxide (TPAOH, Na < 5 ppm, K < 5 ppm) was prepared by ion exchange of TPABr (>99%, synthesis grade, Merck-Schuchardt): A ca. 1.2 M TPABr solution was passed through a column of anionic exchange resin in the OH⁻ form (DOWEX-SBR-P, Dow Chemical). The ion-exchange resin was rinsed free of essentially all Na⁺ and K⁺ with excess amounts of distilled water prior to use. The Na and K concentrations in the TPAOH solution were measured by atomic adsorption as described below. The molarity of the prepared TPAOH was determined by titration with HCl solution. Double distilled water was used in all experiments.

TS-1 Synthesis. Colloidal suspensions of TS-1 were prepared by hydrothermal treatment of synthesis solutions (see Tables 1 and 2) in either polyethylene flasks submerged in a preheated silicone oil bath at 100 °C with reflux under static conditions, hereafter termed type A syntheses, or in Teflon-lined autoclaves that were placed in a preheated oven, termed type B syntheses. A typical type A synthesis was performed as follows:

TEOS was transferred to a polyethylene flask, whereafter a certain amount of TEOT was carefully added and stirred vigorously at ambient temperature. The clear solution was stirred for about 15 min at room temperature, and then an alkali-free aqueous TPAOH solution was added dropwise to the mixture at a rate of about 1 mL/min, thus avoiding the formation of TiO₂ (anatase). The mixture was stirred vigorously for about 1 h until a homogeneous phase was obtained, thus marking the completion of the hydrolysis reaction. The resulting clear synthesis mixture (denoted the precursor solution) was heated in the polyethylene flask for 5–7 days. The reflux columns were capped to prevent the loss of ethanol (formed by the hydrolysis reaction).

In syntheses performed at $T \geq 100$ °C, type B syntheses, ethanol was removed from the precursor solutions by boiling, whereafter water was added to account for H₂O losses. The clear solution was transferred to a Teflon-lined autoclave and heated at various temperatures in the range 100–175 °C for 3–5 days.

A reference sample of colloidal TPA-silicalite-1 was prepared at 100 °C in the presence of ethanol using the type A synthesis procedure described above with the exception that no Ti was added. An amorphous precursor powder was prepared by freeze-drying a clear precursor solution directly after completion of the hydrolysis reaction. A part of this sample was calcined at 550 °C in air for 3 h.

Characterization. The as-synthesized aqueous TS-1 suspensions were purified by centrifugation in a Jouan high-speed centrifuge, Model KR22i, with a relative centrifugal force of 60 000*g* for 1 h. The liquid phase was carefully decanted, and the solid phase was redispersed in double-distilled water by ultrasonic treatment. This rinsing procedure was repeated 3–4 times. Purified and redispersed samples were freeze-dried, and the organic template was removed by calcining samples at 550 °C in air for ca. 3 h.

Particle size analysis of dilute as-synthesized aqueous suspensions of TS-1 was performed using a Brookhaven Instruments ZetaPlus. The use of the light-scattering technique for particle size analysis has been described in detail in a previous report.¹⁵ The Brookhaven Instrument BI200SM light-scattering system (laser power 500 mW) was used to

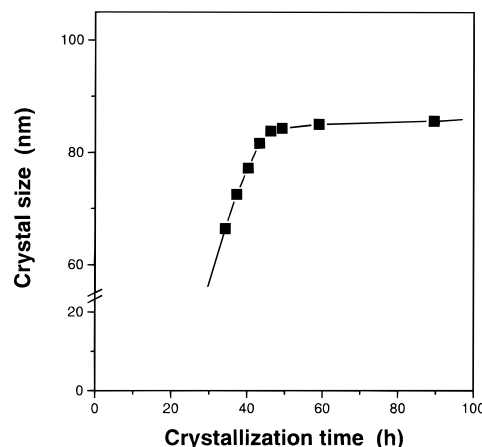


Figure 1. Increase in the average crystal size of TS-1 as a function of crystallization time for run ZT-1.

measure the particle size in a clear precursor solution. Data were collected at scattering angles of 75°, 90°, and 115°. The nonnegative least-squares (NNLS) data analysis method was used to determine the diffusion coefficients. Dust was removed from the precursor solution by filtration through a Gelman Sciences Supor Acrodisc membrane filter, 0.2 μm pore size, prior to the light-scattering measurements.

SEM micrographs were taken with a Philips XL 30 scanning electron microscope (SEM). Dilute aqueous samples of purified suspensions were dried on a glass plate and thereafter coated with a thin carbon film. Crystal phases were identified by X-ray powder diffraction (XRD) with a Philips PW 1710 diffractometer using Cu Kα radiation. Powder samples for XRD analysis were prepared by freeze-drying purified sols followed by calcination of the powder at 550 °C for 3 h in air.

The DRIFT spectra of freeze-dried powder samples were obtained using the KBr wafer technique with a Perkin-Elmer PE 2000 FT-IR spectrometer. Data were collected with 200 scans and a resolution of 4 cm⁻¹ in the frequency range 370–1300 cm⁻¹. UV-vis diffuse reflectance spectra were collected with a Perkin-Elmer Lambda 2S spectrometer using freeze-dried powder samples. The FT Raman spectra were recorded with a Perkin-Elmer PE 1700X NIR FT-Raman spectrometer equipped with a Nd:YAG laser source. Spectra were collected with 200 scans and a resolution of 4 cm⁻¹. Low-frequency FT-Raman spectra with an instrumental resolution of 4.0 cm⁻¹ were recorded at 295 K using a 180° backscattering geometry. The spectra were recorded with a Bruker IFS 66 spectrometer and a Raman module FRA 106 equipped with a continuous Nd:YAG laser (1064 nm, Gaussian line width ~ 10⁻⁵ cm⁻¹).

Specific surface areas of freeze-dried powder samples were measured by N₂ adsorption according to the BET method with a Micromeritics ASAP 2010 surface area analyzer. The samples were outgassed at 200 °C for 5 h in vacuum before measurement. The N₂ adsorption isotherms were recorded at 77 K.

Chemical analysis of the samples was performed with atomic absorption spectroscopy using a Perkin-Elmer Model 3100 atomic absorption spectrometer after dissolving the samples in HF-HCl solutions.

Measurements of the colloidal crystals electrophoretic mobility¹⁶ were carried out using a Laser Zee Meter instrument (PENKEM Model 501). Purified TS-1 sol samples were diluted with a KCl solution to obtain an electrolyte content of 10 mM KCl. The pH of the suspensions was adjusted by the addition of NaOH or HCl solutions. The samples were equilibrated for 2 h at room temperature with stirring. Before measurement, each solution was subjected to ultrasonic treatment for a few minutes, whereafter the pH was measured and a part of the solution was injected into the sample cell to measure the

(14) Persson, A. E.; Schoeman, B. J.; Sterte, J.; Otterstedt, J.-E. *Zeolites* **1995**, *15*, 611.

(15) Schoeman, B. J.; Sterte, J.; Otterstedt, J.-E. *J. Porous Mater.* **1995**, *1*, 185.

(16) Hunter, R. J. *Foundations of Colloid Science*; Clarendon Press: Oxford, 1987.

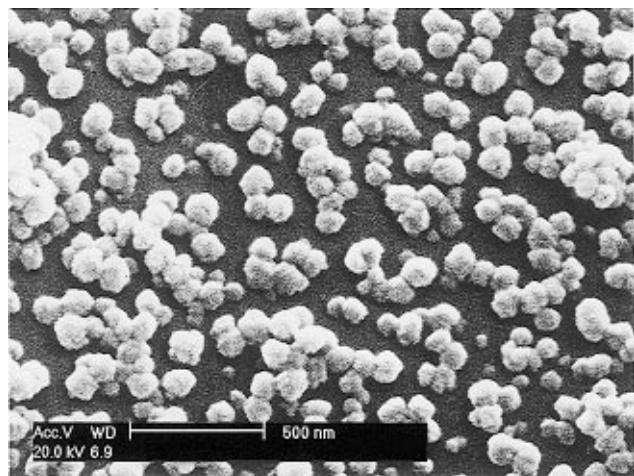


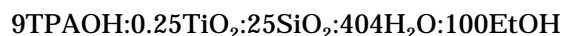
Figure 2. Scanning electron micrograph of the discrete TS-1 crystals in the ultimate product of run ZT-1. Scale bar = 500 nm.

electrophoretic mobility. The ζ potential was calculated from the electrophoretic mobility data with Smoluchowski's equation.¹⁶

Thermogravimetric analysis (TGA) of selected noncalcined samples was performed with a Perkin-Elmer TGA 7 Analyzer. The samples were heated in air at a heating rate of 10 °C/min.

Results and Discussion

1. Synthesis and Characterization of Colloidal Suspensions of TS-1. *1.1 Standard Run.* The synthesis mixture with the molar composition:



termed the standard run and referred to as ZT-1 yields a colloidal suspension of discrete TS-1 crystals after ca. 50 h hydrothermal treatment of the clear hydrolyzed precursor sol at 100 °C (a type A synthesis). XRD analysis, not shown here, of a freeze-dried purified powder sample of ZT-1 showed that the sample consists of a highly crystalline zeolite having the MFI structure, with peak broadening due to the small crystal size. The results of the growth of the crystals, monitored with dynamic light scattering (DLS), are shown in Figure 1. The average DLS crystal size of the ultimate product in experiment ZT-1 is 85 nm. The coefficient of variation (c.v.), a measure of the width of the particle size distribution, is 5.6%. Since the c.v. of the sol is less than 10%, the colloidal suspension can be considered as being "monodisperse".¹⁶ These results are confirmed by the SEM micrograph, (Figure 2).

DRIFT analysis of the product crystals obtained in run ZT-1 (Figure 3a) shows the characteristic absorption bands at 440, 550, and 960 cm^{-1} , normally seen in the DRIFT spectra of the TS-1 phase. The band at 550 cm^{-1} has been assigned as being due to the double rings of tetrahedra in the framework of the MFI structure.¹⁷ Sharp bands at both 550 and 440 cm^{-1} indicate that the colloidal product is a well-crystallized zeolite with the MFI structure, in agreement with the XRD data. The absorption band at 960–970 cm^{-1} , absent in the DRIFT spectrum of calcined ZSM-5, is characteristic of

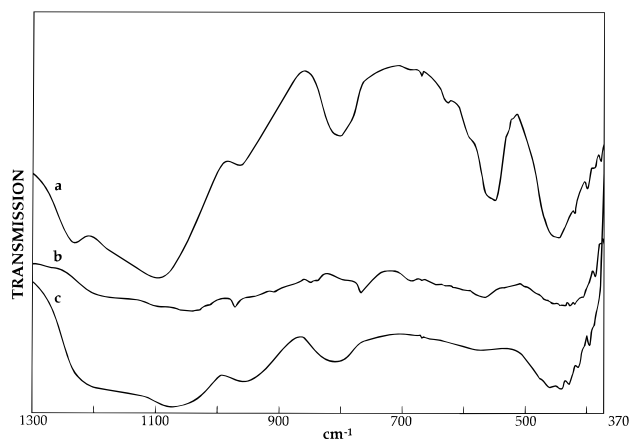


Figure 3. DRIFT spectra of (a) the freeze-dried, purified, and calcined (550 °C, 3 h) product in run ZT-1, (b) the freeze-dried precursor ZD, (c) the freeze dried and calcined (550 °C, 3 h) precursor ZDC.

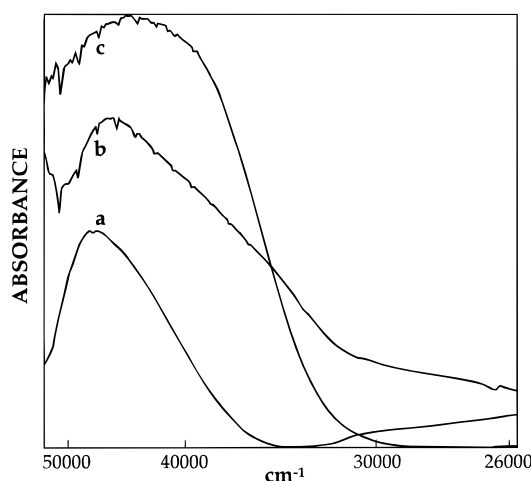


Figure 4. UV-vis diffuse reflectance spectrum of (a) the freeze-dried, purified, and calcined (550 °C, 3 h) product in run ZT-1, (b) the freeze-dried precursor ZD, and (c) the freeze-dried and calcined (550 °C, 3 h) precursor ZDC.

TS-1. According to Boccuti et al.,¹⁸ this band can be attributed to a stretching mode of SiO_4 units adjacent to framework titanium atoms (O_3SiOTi) since the Ti–O–Si bond is more polar than the Si–O–Si bond.

UV-vis is regarded as being a sensitive method to detect framework and extra framework Ti.¹⁹ The strong transition band at ca. 48 000 cm^{-1} evident in the UV-vis spectrum of TS-1 is ascribed as being due to isolated framework Ti(IV) in the tetrahedral coordination.¹⁸ The absorption band at 42 000 cm^{-1} , due to isolated Ti(IV) in an octahedral environment, and absorption bands due to nonisolated octahedrally coordinated Ti(IV) in oxidic clusters, that normally appear at lower frequencies (for example pure anatase that shows an absorption band at ca. 30 500 cm^{-1}), are not evident in the diffuse reflectance UV-vis spectrum of ZT-1, shown in Figure 4a. This would indicate that the Ti in the product of run ZT-1 is tetrahedrally coordinated and the product is free from occluded TiO_2 .

The Raman band at 960 cm^{-1} evident in the Raman spectra of ZT-1 (Figure 5a) is characteristic of 4-fold

(17) Coudurier, G.; Naccache, C.; Vadrine, J. C. *J. Chem. Soc., Chem. Commun.* **1982**, 1413.

(18) Boccuti, M. R.; Rao, K. M.; Zecchina, A.; Leofanti, G.; Petrini, G. *Stud. Surf. Sci. Catal.* **1989**, 48, 133.

(19) Zecchina, A.; Spoto, G.; Bordiga, S.; Ferrero, A.; Petrini, G.; Leofanti, G.; Padovan, M. *Stud. Surf. Sci. Catal.* **1991**, 69, 251.

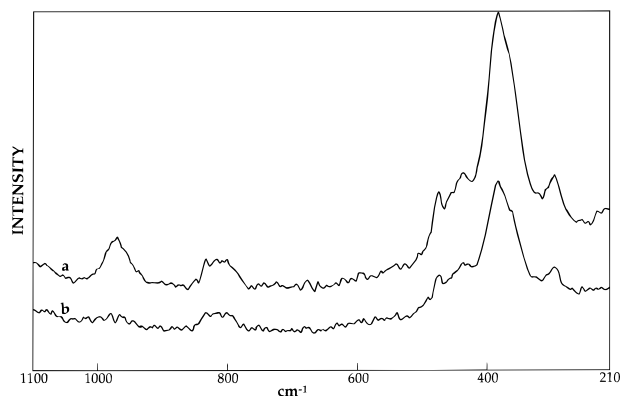


Figure 5. FT Raman spectra of freeze-dried, purified, and calcined (550 °C, 3 h) products in (a) run ZT-1 and (b) silicalite-1.

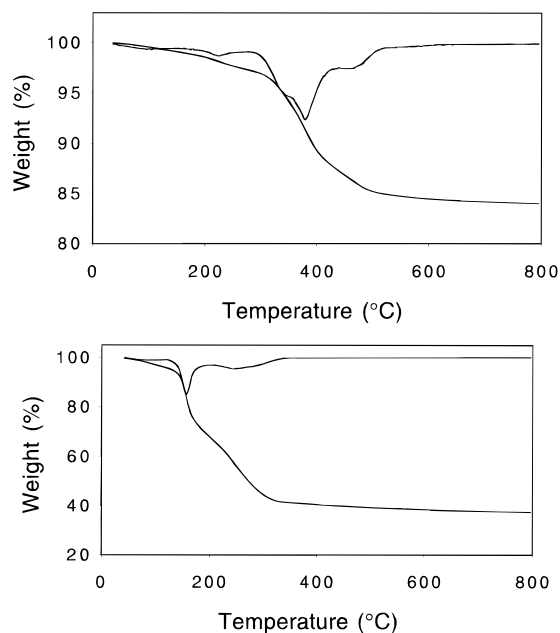


Figure 6. TGA/DTA curve of (a) the purified and freeze-dried product in run ZT-1 and (b) the freeze-dried precursor ZD.

coordinated titanium in the MFI structure. This band has not been observed in the Raman spectra of silicalite-1 or in the B-, Al-, Fe-, or Ga-substituted forms of silicalite or other MFI zeolites.²⁰ Besides the band at 960 cm^{-1} , the spectrum of ZT-1 is similar to the spectrum of the Ti-free reference sample, silicalite-1 (Figure 5b).

The specific surface area of a purified and calcined (550 °C, 3 h) ZT-1 sample calculated using the BET equation is 501 m^2/g . Similar results have been obtained for Ti-free TPA-silicalite-1.¹²

The results of the TGA/DTA analysis of a freeze dried sample of ZT-1 is shown in Figure 6a. The 16% weight loss is the result of the removal of water and organic template decomposition. Due to TS-1's hydrophobic nature, water lost at 100 °C is less than 1%. The small peak at 230 °C may correspond to the decomposition of free template and the surface-adsorbed template—the nonstructural organic template. Endothermic peaks between 330 and 470 °C correspond to the decomposition of occluded template in different pore and channel

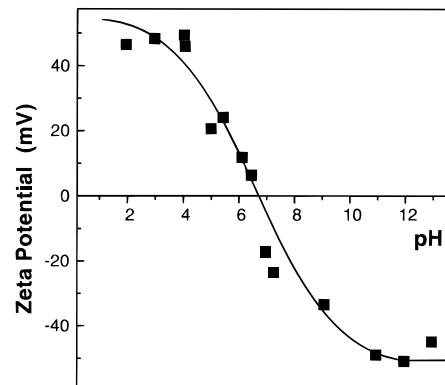


Figure 7. ζ potential of the purified product in run ZT-1 as a function of pH in a 0.01 M KCl medium.

systems. The weight loss above 300 °C was 12.8%. This figure is in agreement with the calculated weight loss, 12.4 wt %, due to the decomposition of organic template in pure silicalite with the unit-cell composition $(\text{TPA-OH})_4-(\text{SiO}_2)_{96}$.

The ζ potential, an important parameter in colloid chemistry, is a measure of surface electric charge and may yield information regarding the stability of a colloidal system.¹⁶ In general, colloidal particles with a high surface electric charge of the same sign will repel each other, thereby maintaining their discrete nature. At lower ζ potentials, closer to the point of zero charge, the attractive forces will dominate over the electrostatic repulsive forces and the colloidal crystals will show a tendency to aggregate. Knowledge of the ζ potential of a colloidal system is therefore very important in the preparation of materials, e.g., catalyst preparation using impregnation methods, the coating of fibers and the preparation of films or membranes. The change in the ζ potential of the colloidal TS-1 crystals as a function of pH is shown in Figure 7. The pH at which the net surface charge is zero, termed the point of zero charge, pH_{pzc} , is at a pH of ca. 6.7. A similar value has been obtained in a previous study dealing with TPA-silicalite-1.²¹ It can be seen that the ζ potential in an acidic environment, $\text{pH} < 4$, is positive, ca. +45 mV, and decreases with increasing pH. For pH values higher than the pH_{pzc} , the ζ potential decreases with increasing pH. The ζ potential reaches a steady value of ca. -50 mV at a $\text{pH} > 10$. The relatively high charge of the crystals at low and high pH values is probably a major factor in the stabilization of the suspensions. Aggregation of the colloidal crystals is observed at intermediate pH values probably due to the absence of electrostatic repulsive forces. It should also be noted that the dependence of ζ potential on pH as seen in Figure 7 for TS-1 is not typical for all molecular sieves. It has been shown that the crystalline aluminosilicates (zeolites) do not have a point of zero charge and hence they are negatively charged in the pH range ca. 4–11. At a pH below ca. 4, the aluminum is leached out from the zeolite, resulting in the destruction of the structure.

1.2. Effect of Si/Ti Ratio in the Synthesis Solution. Type A synthesis runs at 100 °C with various Si/Ti molar ratios in the synthesis solutions are listed in

(20) Pilz, W.; Peuker, Ch.; Tuan, V. A.; Fricke, R.; Kosslick, H. *J. Phys. Chem.* **1993**, *97*, 1037.

(21) Persson, A. E.; Schoeman, B. J.; Sterte, J.; Otterstedt, J.-E. Preparation of Colloidal Suspensions of Silicalite. In *Synthesis of Microporous Materials: Zeolites, Clays, and Nanostructures*; Occelli, M. L., Kessler, H., Eds.; Marcel Dekker: New York, 1996; p 159.

Table 1. Influence of the Si/Ti Molar Ratio in Type A Synthesis Solutions with Molar Compositions $9\text{TPAOH}:x\text{TiO}_2:25\text{SiO}_2:404\text{H}_2\text{O}:100\text{EtOH}$ on Crystal Size, Zeolite Concentration, and Zeolite Si/Ti Molar Ratio

run	TiO ₂ content x	average crystal size (nm)	zeolite concn (g of zeolite/g of sol) $\times 10^2$	zeolite Si/Ti molar ratio
silicalite-1	0	78	<i>a</i>	∞
ZT-1	0.25	85	<i>a</i>	260
ZT-2	0.14	80	8.88	305
ZT-3	0.32	83	<i>a</i>	181
ZT-4	0.46	88	8.04	186
ZT-5	0.95	86	<i>a</i>	167
ZT-6	1.46	99	<i>a</i>	119
ZT-7	1.67	109	7.40	118

^a Not measured.

Table 1. Both the average crystal size and the Ti/Si molar ratio in the products increase with increasing Ti content in the synthesis solutions. The presence of titania in the precursor sols results in slower reaction kinetics; the higher the Ti content in the synthesis mixture, the slower the crystallization. These results are analogous to those obtained in a study of colloidal ZSM-5 when introduction of alumina to a TPA-silicalite-1 precursor also results in a slower crystallization rate and larger product crystals compared to similar runs in the absence of alumina.¹⁴ The increase in the ultimate crystal size with increasing Me (Me = Al, Ti) contents in the synthesis mixture is believed to be due to the decrease in the solubility of the silica. Although the precursor solutions used to synthesize colloidal TS-1 (and ZSM-5¹⁴) appear to be clear homogeneous solutions, the greater part of the silica is present as subcolloidal particles, as will be shown and discussed below. The lower content of soluble silica available for nucleation results in fewer nuclei, and the material available for crystal growth is distributed among fewer particles whose ultimate size is larger than those synthesized in the absence of Me.

DRIFT analyses of TS-1 samples have shown that Ti incorporation increases with increased Ti concentration in the synthesis solutions.²² The absorption band at ca. 960 cm^{-1} , indicative of tetrahedrally coordinated Ti, increases in intensity with increased Ti contents in the synthesis mixture. A maximum incorporation of Ti corresponding to 0.84 mol % Ti (Si/Ti molar ratio = 118), run ZT-7, was obtained with the compositions studied in this work. No extraframework Ti was observed in the UV-vis diffuse reflectance spectra of samples synthesized at 100°C (see Figure 8). Ti analysis of the mother liquid after centrifugation showed that unreacted Ti remained in the mother liquid rather than forming extraframework Ti in the zeolite. The intense Raman band at 144 cm^{-1} , characteristic of the anatase phase and used to detect extraframework Ti in TS-1,^{19,20} is not evident in the Raman spectrum of the product in run ZT-7 (the run with the highest Ti content used in type A syntheses; see Figure 8). The appearance of the Raman spectra is similar to that shown by Pilz et al.,²⁰ in which the absence of anatase is claimed.

1.3. Effect of Si/TPAOH Ratio in the Synthesis Solution. The variation in crystal size due to the TPAOH content in the synthesis solutions is shown in

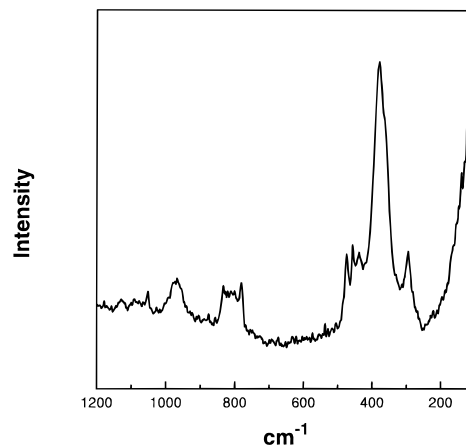


Figure 8. Low-wavelength FT Raman spectrum of the freeze-dried, purified, and calcined (550°C , 3 h) product in run ZT-7.

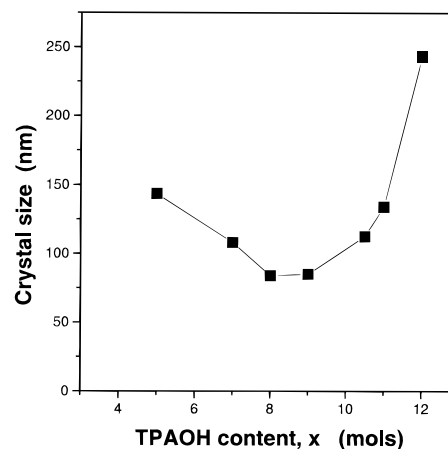
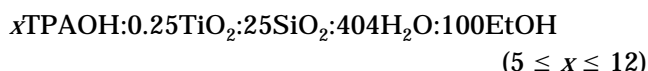


Figure 9. Crystal size of the ultimate product as a function of the TPAOH content in the synthesis mixture with synthesis molar composition $x\text{TPAOH}:0.25\text{TiO}_2:25\text{SiO}_2:404\text{H}_2\text{O}:100\text{EtOH}$ ($5 \leq x \leq 12$).

Figure 9. The compositions of the synthesis solutions were:



The minimum crystal size was obtained for values of x in the range 8–9. The influence of alkalinity on crystal size is thought to be due to differences in nucleation behavior—at the lowest alkalinities (where TPA is limiting) relatively very few nuclei are formed. With increasing alkalinity, the number of nuclei increases until a point at which the solubility of the small particles is such that the number of nuclei decreases. Crystals growing in an environment with an alkalinity below the optimum alkalinity attain larger crystal sizes since the available material for growth is distributed among fewer growth centers. This is also true for those crystals grown in highly alkaline solutions.

1.4. Effect of Water Content in the Synthesis Solution. The influence of diluting the synthesis solution on the ultimate crystal size and the Ti content in the product crystals is shown in Table 2. Dilution results in an increase in the crystal growth rate, the average crystal size, and the Ti-content in the product. The time taken to obtain the ultimate product decreased from ca. 50 h in run ZT-8 (water content corresponding to $x = 404$)

(22) Zhang, G.; Sterte, J.; Schoeman, B. J. *J. Chem. Soc., Chem. Commun.* **1995**, 2259.

Table 2. Influence of the Si/H₂O Molar Ratio in Type A Synthesis Solutions with Molar Compositions 9TPAOH:0.55TiO₂:25SiO₂:xH₂O:100EtOH on Crystal Size and Zeolite Si/Ti Molar Ratio

run	H ₂ O content <i>x</i>	average crystal size (nm)	zeolite Si/Ti molar ratio
ZT-8	404	87	175
ZT-9	1000	142	122
ZT-10	2000	234	67

Table 3. Influence of Crystallization Temperature on the Si/Ti Molar Ratio in the Products Synthesized (Type B Synthesis) Using a Synthesis Mixture Molar Composition 9TPAOH:1.4TiO₂:25SiO₂:404H₂O:100EtOH

temp (°C)	100 ^a	100	125	150	175
Si/Ti molar ratio in the product	150	116	43	37	18

^a Performed in the oil bath at atmospheric pressure (type A synthesis).

to ca. 20 h in run ZT-10 ($x = 2000$). The crystal size increased from 87 nm ($x = 404$) to 234 nm ($x = 2000$). The influence of the water content on the crystal size and the crystal growth rate is not in agreement with the results of Thangaraj et al., who reported that dilution of the synthesis mixture with water in the TS-1 synthesis was found to have little influence on the rate of crystallization.²³ In their work, the synthesis of TS-1 was performed using Ti(OBu)₄ as the titania source. Although the Ti source differs from that used in this work, it is unlikely that this factor can explain this discrepancy. The effect of the water content in the synthesis of colloidal TS-1 is however similar to that observed in the synthesis of colloidal ZSM-5.¹⁴ There may be several reasons for the increased growth rates and crystal sizes upon dilution of the synthesis mixtures with water. Among these, the reduction in solution viscosity, a slight reduction in pH, a redistribution of silica species upon dilution may explain the higher growth rates.

1.5. Effect of Synthesis Temperature—Type B Syntheses. Several type B synthesis runs were performed at different temperatures in autoclaves at autogeneous pressure (see Table 3) using the sol composition



The type A synthesis prepared in the oil bath at 100 °C was performed in the presence of ethanol, and therefore the synthesis solution temperature was between 85 and 90 °C, i.e., the boiling point of the ethanol and water-containing solution. With increasing temperature, ≥ 100 °C, the Ti content in the product increased. The fact that high temperature favors Ti incorporation has also been reported by Bellussi et al.⁸ Figure 10 shows the UV-vis diffuse reflectance spectra of the purified and calcined TS-1 samples prepared at different temperatures. All samples show the absorption bands at ca. 48 000 cm⁻¹ in the UV-vis spectra. Both samples prepared at 100 °C (types A and B syntheses) were pure TS-1 with tetrahedral coordinated Ti(IV) (only one adsorption peak at 48 000 cm⁻¹) without extraframework Ti(IV). Absorption bands in the range 42 000–26 000 cm⁻¹ are present in the spectra of samples synthesized at 125, 150, and 175 °C (spectra c–e in Figure 10, respectively). The maxima of these

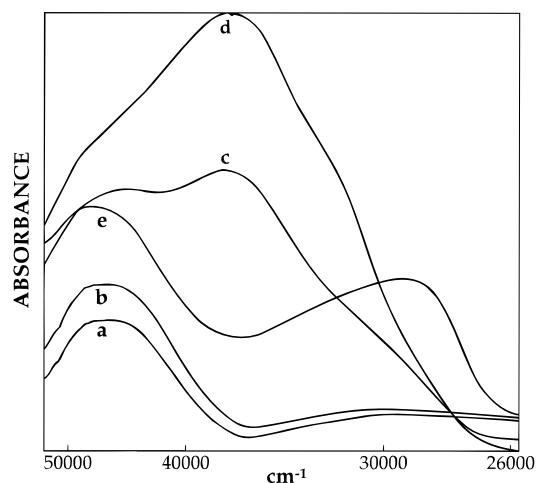


Figure 10. UV-vis diffuse reflectance spectra of freeze-dried, purified, and calcined products (550 °C, 3 h) obtained using a synthesis molar composition 9TPAOH:1.4TiO₂:25SiO₂:404H₂O:100EtOH and synthesized in (a) 100 °C oil bath (type A synthesis), (b) 100 °C autoclave (type B synthesis), (c) 125 °C autoclave (type B synthesis), (d) 150 °C autoclave (type B synthesis), and (e) 175 °C autoclave (type B synthesis).

curves in this range shifts toward lower frequencies with increasing temperature. The absorption bands at lower frequencies, 42 000 cm⁻¹ evident in the spectra c–e are ascribed as being due to nonisolated octahedral coordinated Ti(IV) in oxidic clusters. Pure anatase (TiO₂) (absorption band at ca. 30 000 cm⁻¹) precipitated into the structure in the sample synthesized at 175 °C. Although high temperatures favor low Si/Ti molar ratios in the products, a major part of the Ti is present as nonframework Ti when the Si/Ti molar ratio in the synthesis solution is high.

2. Characterization of the Amorphous Precursor Solution. Previous investigations of the clear homogeneous solutions used for the synthesis of colloidal crystals of TPA-silicalite-1 have shown that subcolloidal particles with a size less than 5 nm exist in suspension following hydrolysis of tetraethoxysilane and prior to hydrothermal treatment.²⁴ The clear titanosilicate precursor solution prepared in this work was studied using the light-scattering technique with a high laser effect. The presence of subcolloidal particles with an average size of 4.8 nm was detected in suspension. To cast more light on the nature of these particles, the precursor solution was freeze-dried to the powder form (denoted sample ZD). At no time was the precursor solution exposed to elevated temperatures, thus minimizing the negative effects of high temperatures. These negative effects include a redistribution of silicate species in solution, redistribution of the particulate silica such that the number of particles decreases at the expense of the growth of the remaining particles (as has been observed during an in situ light-scattering study of the crystallization of silicalite performed at 70 °C²⁴) and the risk of the formation of ordered structures not originally present in suspension prior to the invasive treatment. A portion of the freeze dried powder was calcined in air at 550 °C for 3 h (denoted sample ZDC) thus removing the organic content of the powder.

As may be expected, both samples are XRD amorphous, indicating the absence of any long-range order.

(23) Thangaraj, A.; Eapen, M. J.; Sivasanker, S.; Ratnasamy, P. *Zeolites* **1992**, *12*, 943.

(24) Schoeman, B. J., manuscript in preparation.

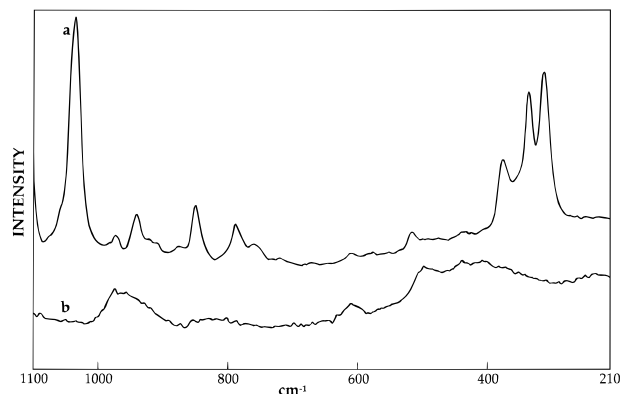


Figure 11. FT-Raman spectra of (a) the freeze-dried precursor ZD and (b) the freeze-dried and calcined (550 °C, 3 h) precursor ZDC.

Indications of short-range order is however evident in the DRIFT spectra of both samples, ZD and ZDC (Figure 3b,c, respectively). DRIFT analysis, considered a more sensitive method for short-range ordering, shows that a weak absorption band in the range 600–550 cm^{-1} is present in both samples. Since the appearance of both the 440 and the $\sim 550 \text{ cm}^{-1}$ absorption bands may indicate the presence of MFI ordered structures, there are indications that the XRD amorphous precursor powder contains structures that could serve as growth centers in the proceeding hydrothermal crystallization of TS-1. As may be expected, the band at $\sim 550 \text{ cm}^{-1}$ in the DRIFT spectrum of sample ZDC is weaker than the same band in the spectra of sample ZD. This is probably due to the partial destruction of the short-range order upon calcination. A relatively strong absorption band at ca. 960 cm^{-1} in the DRIFT spectrum of both samples indicates the presence of $\text{SiO}_4\text{-Ti}$ bridges.¹⁸ This band in the spectrum of sample ZDC is maintained despite calcination, indicating that this structural property is a stable conformation.

The UV-vis diffuse reflectance spectra (Figure 4b,c) shows that the absorption band is rather broad. This indicates that both tetrahedral (absorption at $48\,000 \text{ cm}^{-1}$) and octahedral coordinated Ti (absorption at $<48\,000 \text{ cm}^{-1}$) is present in these samples. No indications of the presence of anatase can be observed in the spectra of either the freeze-dried precursor or the calcined precursor. The Raman spectra of samples ZD and ZDC are shown in Figure 11. The absorption peaks due to the TPAOH molecules (which absorb strongly in the Raman) are clearly visible in the spectrum of the noncalcined sample while they are not present in the spectra of the calcined sample as may be expected. According to Dutta and Puri,²⁵ structurally entrapped TPA detected with Raman is indicative of short-range ordering, thus providing evidence of the presence of MFI precursor units. It is however not possible to assign the peaks in Figure 11a as being due to structurally entrapped TPA entities which otherwise could provide further evidence for the presence of channel structures in the noncalcined precursor powder. The absorption bands evident in Figure 11a are due primarily to TPAOH originally in solution and external surface-adsorbed TPA. If structurally entrapped TPA is present in this sample, their absorption bands will not be visible

since they are masked by the bands due to the free TPA. Of interest however is the absorption peak at ca. 970 cm^{-1} in the spectra of sample ZDC which is due to tetrahedrally coordinated Ti in accordance with the DRIFT results presented above. The absorption peaks due to the inorganic components of the MFI phase, at 380, ca. 800, and $>1000 \text{ cm}^{-1}$, may be present as weak bands in the spectra of sample ZDC since the MFI framework absorbs only weakly in the Raman.²⁵ The possible presence of these bands is not however sufficient evidence for the existence of the MFI framework structure. The results presented above are interpreted as being due to the simultaneous hydrolysis of the TEOT and the TEOS in the presence of TPAOH and the condensation of the species generated. The condensation step includes the incorporation of a part of the titanium as tetrahedrally coordinated Ti while the remaining Ti is present as octahedrally coordinated Ti. Although the absorption bands in the DRIFT, Raman and UV-vis spectra provide evidence of the presence of short-range order in the subcolloidal particles, the relationship between these species and the nucleation and growth of TS-1 is not fully understood.

The specific surface area of the calcined precursor is $705 \text{ m}^2/\text{g}$ and the pore volume calculated by the Micro Pore method^{26,27} is $0.30 \text{ cm}^3/\text{g}$. Furthermore, the pore size distribution shows that micropores are present in the sample with an average hydraulic radius of 2.8 \AA . It should be noted that the sizes of the 10-member intersecting rings in silicalite-1 are 5.7×5.1 and 5.4 \AA .²⁸ The presence of micropores may be interpreted as being due to the existence of short-range ordered inorganic-organic structures in which the organic structure-directing agent, TPAOH, is entrapped before removal by calcination. The results of the TGA/DTA analysis of sample ZD shown in Figure 6b indicate a weight loss of 56% below $300 \text{ }^\circ\text{C}$ and 7% above $300 \text{ }^\circ\text{C}$. The former result is ascribed as being due to the decomposition of free TPAOH as well as (external) surface-adsorbed TPA cations. The latter result is most likely due to the decomposition of structurally entrapped TPA cations. In view of the spectroscopic results presented above and the N_2 -adsorption analysis, it appears to be a reasonable assumption that the TPAOH molecules are present in the interior of the particles via their incorporation during the hydrolysis/condensation step. Removal of these organic structure-directing agents by calcining yields the microporous structure as indicated from the N_2 -adsorption analysis.

In conclusion, the results presented above indicate that the subcolloidal particles formed during the room-temperature hydrolysis of tetraethoxysilane and tetraethoxy titanate are not simply amorphous siliceous particles but rather particles that do possess some form of short-range order.

Conclusions

Stable colloidal suspensions of discrete TS-1 crystals have been prepared from clear titanosilicate precursor

(26) Brunauer, S.; Mikhail, R. Sh.; Bodor, E. E. *J. Colloid Interface Sci.* **1967**, *24*, 451.

(27) Mikhail, R.; Brunauer, S.; Bodor, E. E. *J. Colloid Interface Sci.* **1968**, *24*, 45.

(28) Szostak, R. *Handbook of Molecular Sieves*; Van Nostrand Reinhold: New York, 1992.

(25) Dutta, P. K.; Puri, M. *J. Phys. Chem.* **1987**, *91*, 4329.

solutions within a wide temperature range. Although higher crystallization temperatures, $>100^{\circ}\text{C}$, favor products with a low Si/Ti molar ratio, these temperatures also favor the formation of octahedrally coordinated Ti and extraframework Ti as well as larger crystals. Lower temperatures on the other hand favor smaller crystals, $<100\text{ nm}$, with a maximum Ti content of 0.84 mol % present solely as tetrahedrally coordinated Ti. Low water contents in the precursor mixtures favor the crystallization of smaller crystals, but the reaction kinetics are slower than those observed in dilute mixtures. The minimum crystal size obtained in this work was in the range 80–90 nm using the optimum TPAOH/SiO₂ molar ratio of ca. 0.34.

Dynamic light-scattering results showed that subcolloidal particles with an average particle size of 4.8 nm

exist in the precursor solution prepared at room temperature prior to hydrothermal treatment. Preliminary investigations of the freeze-dried precursor indicate the presence of structures with a short-range order.

Acknowledgment. The support of this research by the Swedish Research Council for Engineering Sciences (TFR) is gratefully acknowledged. The authors would like to thank Mr. A. Persson, Royal Institute of Technology, Sweden for performing the TGA/DTA analyses and Dr. Per Jacobsson, Umeå University, Sweden for recording the Raman spectra in the low-wavelength region.

CM960298L